

# Theoretical studies on hydrogen bonding in hydroxylamine clusters and liquid

Kritsana Sagarik

*School of Chemistry, Institute of Science, Suranaree University of Technology, Nakhon Ratchasima, Thailand*

Received 5 February 1998; accepted 24 July 1998

## Abstract

Structures and interaction energies of dimers and trimers of hydroxylamine ( $\text{NH}_2\text{OH}$ ) were investigated using an intermolecular potential derived from the test-particle model (T-model). The T-model results were examined using ab initio calculations at various levels of accuracy, ranging from MP2/6-311G(d,p) to MP2/6-311++G(2d,2p) for the dimers, as well as from MP2/6-31G(d,p) to MP2/6-311++G(2d,2p) for the trimers. Both T-model and MP2 calculations confirmed that a cyclic arrangement of O–H $\cdots$ N hydrogen bonds (H-bonds) represents the absolute minimum energy geometry of the dimers. Several local minimum energy geometries were suggested based on the T-model and MP2 results. For the trimers, the T-model and MP2 predicted a slightly different absolute minimum energy geometry. The T-model preferred a compact H-bonded structure, whereas MP2 with the largest basis set preferred a stacked H-bond arrangement. Ab initio calculations at the SCF/6-311++G(2d,2p) level showed that the effects of electron correlation play an important role in the association of compact H-bonded clusters. Some properties of liquid  $\text{NH}_2\text{OH}$  were investigated based on the T-model potential. Molecular Dynamics (MD) simulations were performed for the liquid at 318 and 329 K. MD results suggested a slightly higher possibility of finding the O–H $\cdots$ O H-bond, compared to the O–H $\cdots$ N H-bond in the liquid. There was no direct evidence showing the existence of cyclic dimers in the liquid. © 1999 Elsevier Science B.V. All rights reserved.

*Keywords:* Ab initio; Dimer; Hydroxylamine; Liquid; Trimer

## 1. Introduction

Structures, energetics and dynamics of hydroxylamine ( $\text{NH}_2\text{OH}$ ) dimer have been investigated in the past 10 years, using various spectroscopic and computational methods [1–11]. Consisting of both O–H and N–H groups in the same molecule, clusters of  $\text{NH}_2\text{OH}$  could be formed using several types of hydrogen bonds (H-bonds), e.g. O–H $\cdots$ N, O–H $\cdots$ O, N–H $\cdots$ N and N–H $\cdots$ O. Yeo et al. [1,4,6] investigated H-bonds in  $(\text{NH}_2\text{OH})_2$ , as well as in  $\text{NH}_2\text{OH}-\text{NH}_3$ , and  $\text{NH}_2\text{OH}-\text{H}_2\text{O}$ , using matrix-isolation infrared (IR)

spectroscopy and ab initio calculations with the 6-31G(d,p) basis set. Ab initio results showed the absolute and at least three local minimum energy geometries on the dimer potential energy surface. A six-membered cyclic structure with two identical O–H $\cdots$ N H-bonds was reported to represent the most stable structure in the gas phase [1]. The result was supported by an analysis of the observed bands in the IR spectra [7]. Based on the shifts of the wavenumbers of the H-bonded O–H and N–H stretching absorption bands, it was pointed out in [6] that the O–H $\cdots$ N H-bond is stronger than the O–H $\cdots$ O and N–H $\cdots$ N H-bonds, respectively. It was also noted in [4] that the N–H $\cdots$ O H-bond is the least favourable

*E-mail address:* kritsana@ccs.sut.ac.th (K. Sagarik)

for the dimer. The N–H···O H-bond had been, therefore, excluded in further investigations.

Michopoulos et al. [10] presented an intermolecular potential function to describe the interaction between two NH<sub>2</sub>OH molecules. The potential energy function was derived based on ab initio calculations with a supermolecular approach. The SCF-ECP (self-consistent field-effective core potential) method was employed with a DZP (double zeta plus one polarization function) basis set for heavy atoms. With special emphasis on the six-membered cyclic structure and some selected H-bonded configurations, 658 energy values were computed, from which the absolute and four local minimum energy geometries were verified with larger basis set calculations, as well as with higher level of theory calculations by the CEPA (Coupled Electron Pair Approximation) method. It was pointed out that, although the absolute interaction energies computed from the SCF-ECP method were not accurate, the relative stability order for the dimers was quite well preserved, in comparison with the CEPA results. All the SCF-ECP interaction energies were fitted to an analytical potential energy function, for which the potential parameters were determined. The dipole moment deduced from the fitted fractional atomic charges was reported to be 1.16 D, compared to the experimental value of  $0.59 \pm 0.05$  D [12]. The intermolecular potential energy function was applied in Monte Carlo (MC) simulations of liquid at 318 K [11]. It turned out that the average potential energy per molecule derived from MC was rather low. In order to obtain a more realistic potential energy of the liquid, the authors had to include some cut-off distance in the potential function. This might be evidence showing the incompleteness of the potential energy surface, especially in the repulsive regions. Since the Basis Set Superposition Error (BSSE) was not corrected in the previous work [10], it could also have made a contribution in the average potential energy of the liquid.

In the present study, an intermolecular potential to describe the interaction between NH<sub>2</sub>OH molecules was constructed using the test-particle model (T-model) [13]. The reported equilibrium structures of the dimers were reinvestigated based on the T-model potential. Since only three dimeric forms have been discussed in detail so far [1–11], the T-model potential was applied in searching for other

possible equilibrium dimer structures in the gas phase. For the first time, the structures and energetics of the trimers in the gas phase were systematically investigated based on the T-model potential. In order to examine the T-model results, some lowest-lying energy geometries predicted by the T-model potential were examined using ab initio calculations at various levels of accuracy. The T-model potential was applied in the calculations of properties of liquid NH<sub>2</sub>OH at 318 and 329 K, using Molecular Dynamics (MD) simulations. The results are discussed in comparison with the previous MC results [11], as well as with available experimental data on the same and similar systems.

## 2. The test-particle model (T-model)

In previous publications [14–20], the T-model had been used in the construction of intermolecular potentials of various chemical systems, ranging from weakly associated molecules, such as NH<sub>3</sub> [14], CHClF<sub>2</sub> [15], CS<sub>2</sub>, CO<sub>2</sub> [16] and N<sub>2</sub> [17], to strongly H-bonded systems, such as NH<sub>2</sub>COH [18], HF and HCN [19]. The computed T-model potentials had been tested and applied successfully in the investigation of various gas and liquid properties. Since the T-model includes the dispersion energy in an approximate way, it was also applied satisfactorily in the studies of dimers of heterocyclic aromatic compounds, such as pyridine [20] and the base pairs of DNA [19]. The most recent publication on phenol [21] confirmed that the T-model potentials are quite suitable for the investigation of structures and energetics of large interacting systems, in which both H-bonding and  $\pi$ – $\pi$  interaction play a dominant role. The derivation of the T-model has been presented in detail elsewhere [13]. Here, only some relevant aspects will be briefly summarized.

In the T-model, the interaction energy ( $\Delta E$ ) between molecules A and B is written as a sum of the first-order interaction energy ( $\Delta E_{\text{SCF}}^1$ ) and a higher-order term ( $\Delta E^r$ ).

$$\Delta E = \Delta E_{\text{SCF}}^1 + \Delta E^r \quad (1)$$

$\Delta E_{\text{SCF}}^1$  accounts for the exchange repulsion and electrostatic energy contributions. It is computed from ab initio calculations [13] and takes the following

Table 1  
Parameters for the T-model potential of NH<sub>2</sub>OH. Values are in atomic units<sup>a</sup>

Atom	Atom	$A_{ij}$	$B_{ij}$	Atom	$q_i$
N	N	90.246658	1.974382	N	-0.7447
O	N	139.808960	2.135996	O	-0.4482
H <sup>N</sup>	N	7.657971	1.867015	H <sup>N</sup>	0.3836
H <sup>O</sup>	N	7.494500	1.970678	H <sup>O</sup>	0.4257
O	O	234.172897	2.326429		
H <sup>N</sup>	O	9.561495	2.010890		
H <sup>O</sup>	O	9.466287	2.131662		
H <sup>N</sup>	H <sup>N</sup>	0.838114	1.770723		
H <sup>O</sup>	H <sup>N</sup>	0.731122	1.863703		
H <sup>O</sup>	H <sup>O</sup>	0.628205	1.966987		

<sup>a</sup>  $\mu = 0.68$  D; H<sup>N</sup> = N-hydrogen; H<sup>O</sup> = O-hydrogen.

form:

$$\Delta E_{SCF}^1 = \sum_{i \in A} \sum_{j \in B} \left[ A_{ij} \exp(-B_{ij} R_{ij}) + \frac{q_i q_j}{R_{ij}} \right] \quad (2)$$

where  $A_{ij}$  and  $B_{ij}$  are the potential parameters and  $R_{ij}$  are the site–site distances. The exponential term in Eq. (2) represents the size and shape of the interacting molecules A and B. The point charges ( $q_i$  and  $q_j$ ) are obtained from the requirement that a point-charge model reproduces the electrostatic potentials of molecules of interest. In our previous study [20], we showed that the potential derived (PD) charges [22] are also applicable. In the present study,  $q_i$  and  $q_j$  for NH<sub>2</sub>OH were determined by a fit of the electrostatic potentials at points selected according to the CHelpG scheme [23]. The electrostatic potentials used in the fit were derived from ab initio calculations at the MP2/6-311G(d,p) level of theory. About 5300 electrostatic energy values were employed in the fit of the atomic charges. The dipole moment computed from the CHelpG point charges was 0.68 D, in comparison with the experimental value of  $0.59 \pm 0.05$  D [12].

The higher-order energy contributions,  $\Delta E^r$  in Eq. (1), could be determined by a calibration of the incomplete potential to the experimental or theoretical properties, related to the intermolecular interaction, such as the second virial coefficients (B(T)), dimerization energies or potential energies of liquid etc.  $\Delta E^r$  represents the dispersion and polarization energy contributions to the intermolecular potential. It takes

the following form:

$$\Delta E^r = - \sum_{i \in A} \sum_{j \in B} C_{ij}^6 F_{ij}(R_{ij}) R_{ij}^{-6} \quad (3)$$

where

$$F_{ij}(R_{ij}) = \exp\left[-(1.28R_{ij}^0/R_{ij} - 1)^2\right], \quad (4)$$

$$R_{ij} < 1.28R_{ij}^0 = 1, \text{ elsewhere}$$

and

$$C_{ij}^6 = C_6 \frac{3}{2} \frac{\alpha_i \alpha_j}{(\alpha_i/N_i)^{1/2} + (\alpha_j/N_j)^{1/2}}, \quad (5)$$

$R_{ij}^0$  in Eq. (4) are the sum of the van der Waals radii of atoms.  $\alpha_i$  and  $N_i$  in Eq. (5) denote the atomic polarizability and the number of valence electrons of the corresponding atom, respectively.  $F_{ij}(R_{ij})$  is a damping function introduced to correct the behavior of  $R_{ij}^{-6}$  at short  $R_{ij}$  distance. Eq. (5) is the Slater–Kirkwood relation. Only  $C_6$  in Eq. (5) is unknown. Since there was no appropriate experimental data available for NH<sub>2</sub>OH,  $C_6$  was determined in the present study by calibration of the incomplete T-model potential with the dimerization energy. The value of  $C_6$  was determined to be 1.24. The derivation of  $C_6$  will be explained in detail in the next section.

The geometry of NH<sub>2</sub>OH was taken from [24] and kept constant throughout the calculations. The computed T-model parameters are listed in Table 1, together with the CHelpG charges on atoms. H<sup>N</sup> and H<sup>O</sup> in Table 1 label N-hydrogen and O-hydrogen of NH<sub>2</sub>OH, respectively.

### 3. NH<sub>2</sub>OH dimers and trimers

The T-model potential computed in the previous section was employed in the calculations of equilibrium structures and interaction energies of (NH<sub>2</sub>OH)<sub>2</sub>. A minimization routine was employed in searching minimum energy geometries of (NH<sub>2</sub>OH)<sub>2</sub>. Starting from randomly generated dimer structures, the absolute and several local minimum energy geometries were located. Some lowest-lying energy geometries are shown in Fig. 1, together with the corresponding interaction energies and some characteristic atom–atom distances. The atom–atom

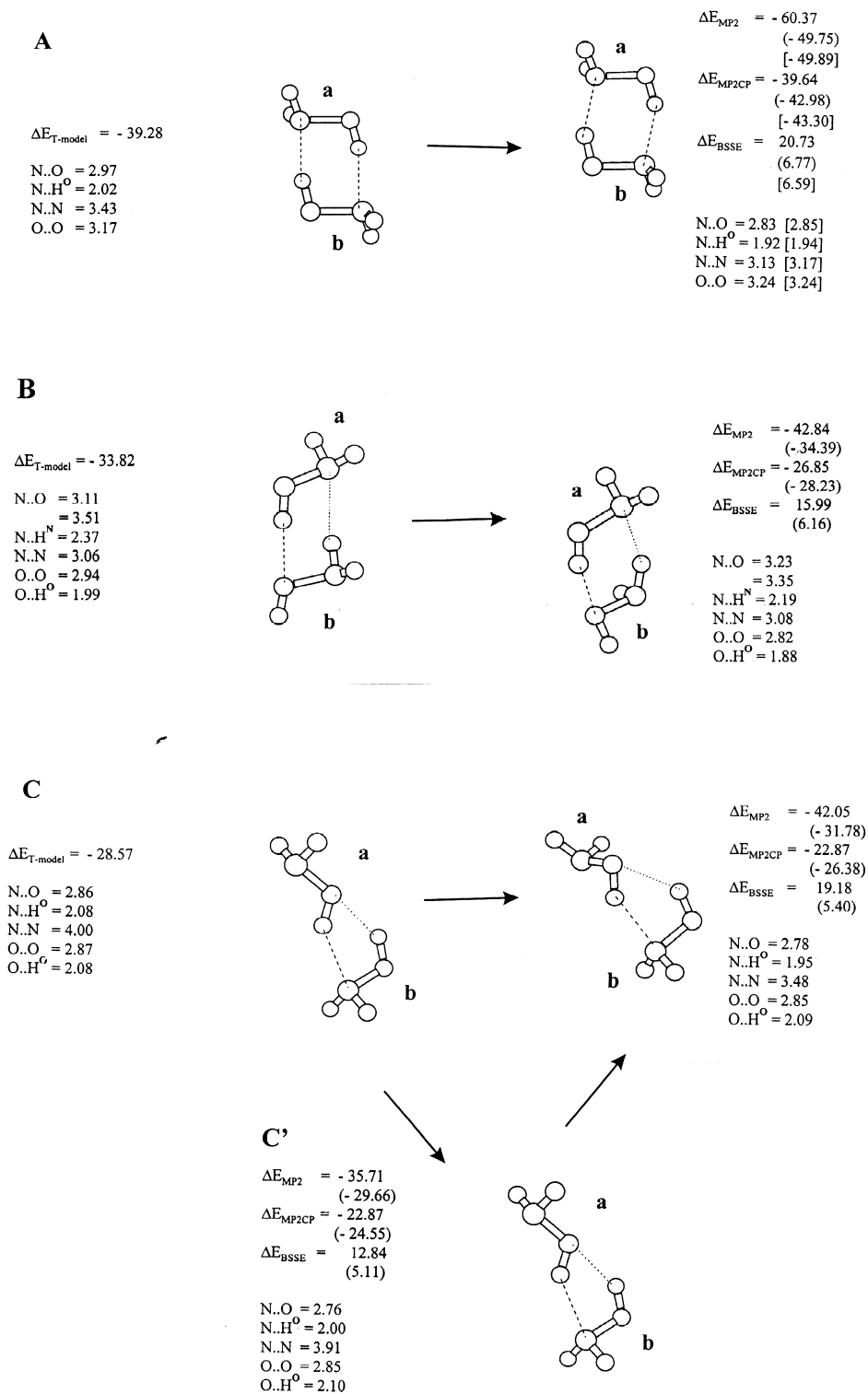


Fig. 1

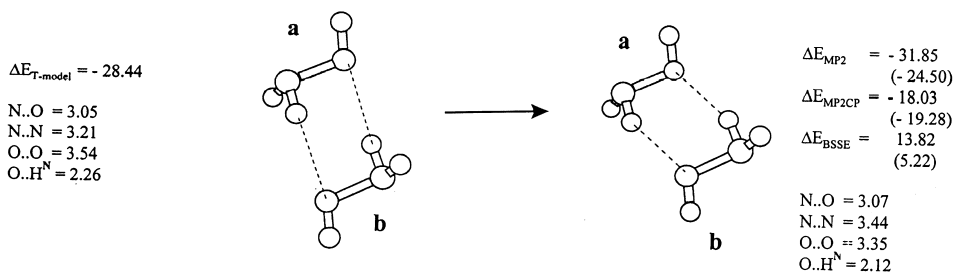
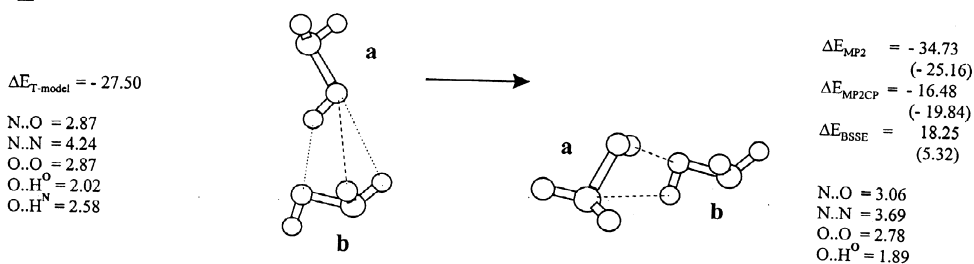
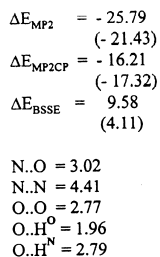
**D****E****E'**

Fig. 1. Absolute and local minimum energy geometries of  $(\text{NH}_2\text{OH})_2$  obtained from the T-model potential, compared with those from MP2. Energy values are in kJ/mol and atom–atom distances in Å. (.....) values derived from MP2/6-311++G(2d,2p) using the 6-311 G(d,p) optimized geometries. [.....] values optimized based on MP2/6-31 1++G(2d,2p).

distances will be used in the discussion of the structure of liquid in Section 4.

In order to examine the T-model results, the equilibrium structures in Fig. 1 were reoptimized using ab initio calculations at the MP2/6-311G(d,p) level of

accuracy. The basis set used is slightly larger than that employed in [1]. Starting from the dimer structures in Fig. 1, geometry optimizations were carried out by keeping the monomer geometry fixed. Traditional Z-matrices [25] of internal coordinates

were used to describe the structures of the dimers. Six variables in the  $Z$ -matrix were optimized using the Berny algorithm [26], included in Gaussian 94 [27]. The counterpoise corrections [28] of BSSE were made only for the newly optimized structures. The optimized dimer structures and the corresponding MP2 interaction energies, both with and without counterpoise corrections, are included in Fig. 1. Some selected atom–atom distances are also reported in Fig. 1 for comparison. The discussion on the interaction energies will be made based on the counterpoise corrected values ( $\Delta E_{\text{MP2CP}}$ ).  $\Delta E_{\text{BSSE}}$  in Fig. 1 is just the difference between  $\Delta E_{\text{MP2CP}}$  and  $\Delta E_{\text{MP2}}$ .

A remark should be made here on the derivation of  $C_6$  in Eq. (5). From our experiences [14,15,18–21], the values of  $C_6$  were close to 1 in many cases. Therefore, the value of  $C_6$  was initially set to 1 for  $\text{NH}_2\text{OH}$ . The T-model potential with  $C_6 = 1$  predicted a six-membered cyclic structure, similar to dimer A in Fig. 1, to be the absolute minimum energy geometry. Starting from this dimer structure, MP2/6-311G(d,p) and the optimization routine in Gaussian 94 located a minimum energy geometry close to the starting geometry, with  $\Delta E_{\text{MP2CP}}$  of  $-39.64$  kJ/mol. The  $C_6$  parameter had been increased from 1 until the absolute minimum energy geometry possessed the interaction energy close to the  $\Delta E_{\text{MP2CP}}$  value. The optimal value of  $C_6$  was found to be 1.24, with the interaction energy ( $\Delta E_{\text{T-model}}$ ) of  $-39.28$  kJ/mol (see dimer A in Fig. 1).

The O–H $\cdots$ N H-bond distance of dimer A was computed to be 2.97 Å. The value is slightly larger than the MP2 result. The T-model potential predicted another six-membered cyclic structure (dimer B in Fig. 1) to be a stationary point. It is 5.46 kJ/mol less stable than dimer A. The O–H $\cdots$ O and N–H $\cdots$ N H-bond distances were computed to be 2.94 and 3.06 Å, respectively. The O $\cdots$ H<sup>O</sup> and N $\cdots$ H<sup>N</sup> distances were 1.99 and 2.37 Å, respectively. Starting from dimer B, Gaussian 94 predicted a similar dimer structure to be a local minimum. The MP2 result showed slightly smaller  $\angle\text{N}\cdots\text{H}-\text{N}$  and  $\angle\text{O}-\text{H}\cdots\text{O}$ , compared with the T-model results.  $\Delta E_{\text{MP2CP}}$  of dimer B was  $-26.85$  kJ/mol, with the O $\cdots$ H<sup>O</sup> and N $\cdots$ H<sup>N</sup> distances of 1.88 and 2.19 Å, respectively.

The T-model potential also predicted a five-membered cyclic structure, in which the oxygen atom in one molecule acts simultaneously as proton

acceptor and donor H-bonding at the oxygen and nitrogen atoms of the other molecule (see dimer C in Fig. 1). Dimer C possesses  $C_s$  symmetry and is about 5.25 kJ/mol less stable than dimer B. Starting from dimer C, the optimization routine in Gaussian 94 generated a slightly different H-bonded structure. The  $\angle\text{N}-\text{O}\cdots\text{N}-\text{O}$  dihedral angle of the newly optimized dimer is about  $80^\circ$ , compared with nearly  $0^\circ$  in dimer C. In order to investigate the relative stability of these two configurations, an additional geometry optimization was made using Gaussian 94. Starting from dimer C, the geometry optimization was carried out by constraining the dimer structure to  $C_s$  symmetry. The newly optimized structure is dimer C in Fig. 1. The interaction energy of dimer C is the same as the unconstrained optimized geometry.

The T-model potential predicted a dimer structure with cyclic arrangement of two N–H $\cdots$ O H-bonds to be another local minimum energy geometry (see dimer D in Fig. 1).  $\Delta E_{\text{T-model}}$  of dimer D is slightly higher than dimer C,  $-28.44$  kJ/mol. Both N–H $\cdots$ O H-bonds in dimer D are identical and almost linear. Both N–H $\cdots$ O distances are 3.05 Å. Starting from dimer D, a similar dimer structure was located by Gaussian 94, with  $\Delta E_{\text{MP2CP}}$  of  $-18.03$  kJ/mol. It should be noted that, for dimers A, B and C, the T-model and MP2 results agree well with those reported by Yeo et al. [1]. However, the present study suggested that dimer D could also be one of the local minima on the energy surface.

The T-model potential predicted a bifurcated-cyclic structure, with  $C_s$  symmetry, to be another stationary point, dimer E in Fig. 1. For dimer E, the O–H group of a molecule acts simultaneously as proton donor and acceptor binding at the oxygen atom and both hydrogen atoms of the other molecule.  $\Delta E_{\text{T-model}}$  in this case is  $-27.50$  kJ/mol. Starting from dimer E, Gaussian 94 suggested another five-membered cyclic structure to be a local minimum. This dimer structure is represented by a cyclic arrangement of the O–H $\cdots$ O and O–H $\cdots$ N H-bonds, with  $\Delta E_{\text{MP2CP}}$  of  $-16.48$  kJ/mol. Starting from the geometry of dimer E, another geometry optimization was carried out by constraining the dimer structure to  $C_s$  symmetry. The minimum energy geometry was found to be dimer E' in Fig. 1, with the interaction energy slightly higher than the unconstrained optimized geometry.

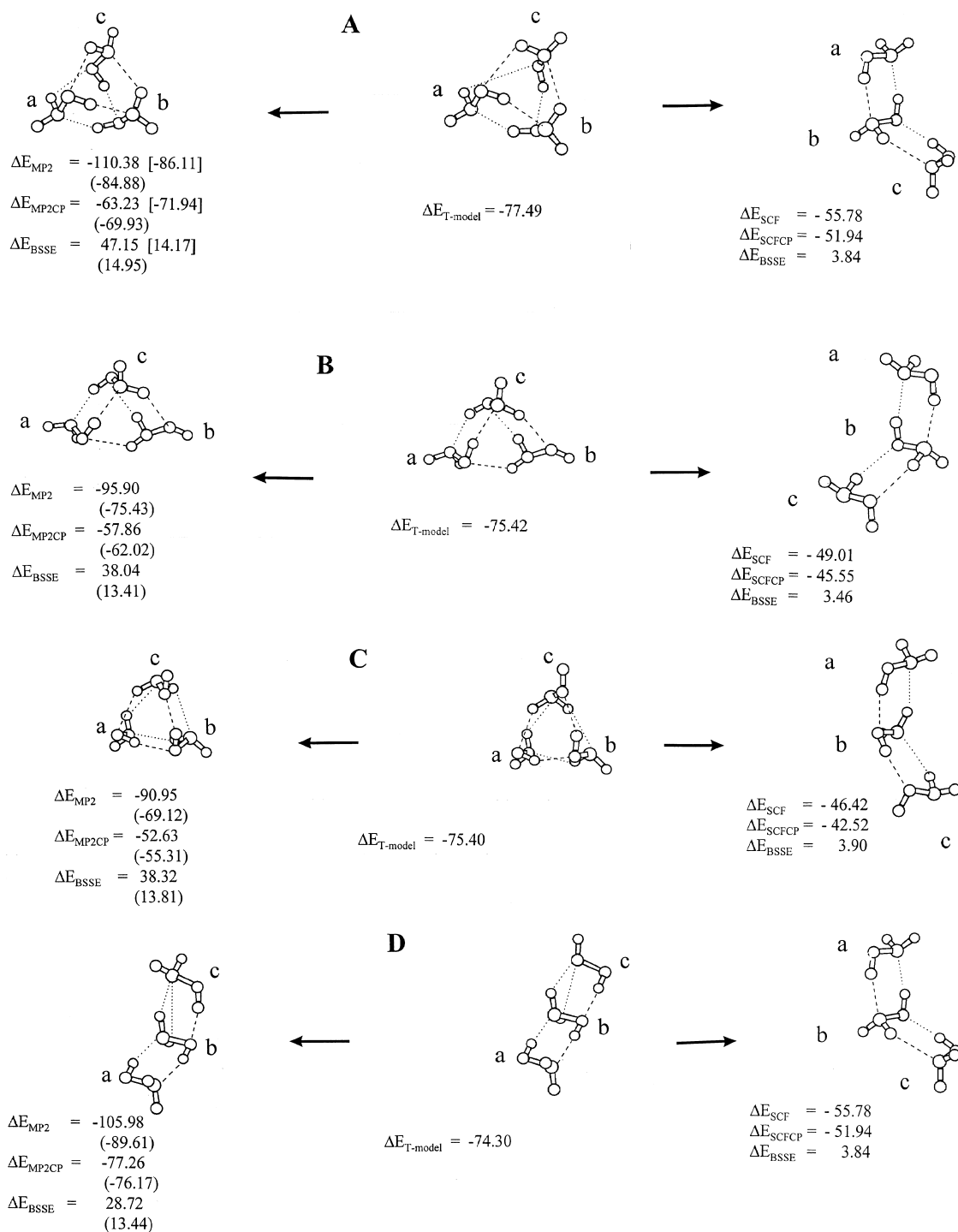


Fig. 2

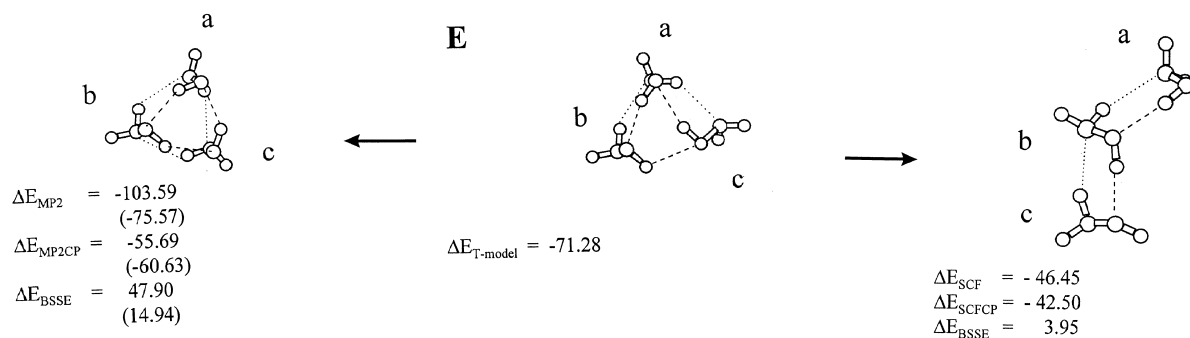


Fig. 2. Energy optimized  $(\text{NH}_2\text{OH})_3$  obtained from the T-model potential, compared with the those from MP2 and SCF. Energy values are in kJ/mol and atom–atom distances in Å. (·····) values derived from MP2/6-311++G(2d,2p) using the 6-31G(d,p) optimized geometries. [·····] values optimized based on MP2/6-311++G(2d,2p).

Based on the interaction energies discussed above, the stability orders for the dimers can be summarized as:

T-model:  $A > B > C \cong D > E$

MP2:  $A > B \cong C > E > D$

MP2CP:  $A > B > C > D > E$

Some remarks should be made here on the MP2/6-311G(d,p) results.  $\Delta E_{\text{BSSE}}$  reported in Fig. 1 are still considerably large and anisotropic for MP2/6-311G(d,p). They are ranging from 20.73 kJ/mol in dimer A to 9.58 kJ/mol in dimer E'. The standard deviation of  $\Delta E_{\text{BSSE}}$  in this case is 3.94 kJ/mol. Based on the above results and the facts that the counterpoise correction yields only the upper boundary of the interaction energies, it is reasonable to expect that the reported stability orders derived from MP2 and MP2CP could be changed if the size of the basis set was increased. In order to check the validity of the above stability orders, a further investigation was made. Dimer A was selected as a test case, since it possesses the largest  $\Delta E_{\text{BSSE}}$ . Starting from the MP2/6-311G(d,p) optimized geometry in Fig. 1, another geometry optimization was carried out at the MP2/6-311++G(2d,2p) level of accuracy. Addition of more polarization functions, as well as diffuse functions, was aimed at reducing  $\Delta E_{\text{BSSE}}$  and, at the same time, improving the description of H-bonds. The newly optimized geometry was, as expected, almost identical to the starting geometry, see the values in square brackets in Fig. 1. The geometry optimization

in this case did not significantly lower the interaction energy, only about 0.3 kJ/mol. MP2/6311++G(2d,2p) yielded much smaller  $\Delta E_{\text{BSSE}}$ , about 14 kJ/mol lower than that of MP2/6-311G(d,p). These results suggested that the geometry optimization could be made with acceptable accuracy using MP2/6-311G(d,p) and only a single MP2/6311++G(2d,2p) calculation on the optimized geometry is required to improve the interaction energy.

Based on the above information, another set of MP2/6-311++G(2d,2p) calculations was made for all the MP2/6-311G(d,p) optimized structures. The energy values are given in parentheses in Fig. 1. The stability orders in this case are:

MP2:  $A > B \cong C > E > D$

MP2CP:  $A > B > C > E \cong D$

As seen in Fig. 1,  $\Delta E_{\text{BSSE}}$  are significantly reduced and become more isotropic for MP2/6-311++G(2d,2p), ranging from 4.11 to 6.77 kJ/mol for dimers E' and A, respectively. The standard deviation of  $\Delta E_{\text{BSSE}}$  is reduced to 0.84 kJ/mol in this case.

The T-model potential was further applied in the investigation of equilibrium structures and interaction energies of  $(\text{NH}_2\text{OH})_3$ . In this case, there were many possibilities to combine three  $\text{NH}_2\text{OH}$  molecules to form H-bonded complexes. Based on the T-model potential, equilibrium structures of  $(\text{NH}_2\text{OH})_3$  were searched using the same procedure as carried out for the dimers. The absolute and several local minimum energy geometries were generated. Only the first five

lowest-lying energy geometries are shown in Fig. 2, together with the interaction energies. In order to make the discussion on the trimer structures simple, each  $\text{NH}_2\text{OH}$  was labeled with **a**, **b** and **c** and H-bonds were represented by dashed lines.

In order to examine the T-model results, all the equilibrium structures shown in Fig. 2 were reoptimized using ab initio calculations at the MP2 level. The same procedure as in the case of the dimers was employed for the trimers. Starting from the structures obtained based on the T-model potential, the Berny optimization routine in Gaussian 94 was applied to locate the nearest stationary points on the potential energy surface. Twelve variables in the Z-matrix were allowed to change in the optimizations. In order to maintain reasonable CPU time, the basis set used in this case was reduced to 6-31G(d,p) in the MP2 calculations. A single point counterpoise correction [28] was applied for the newly optimized structures. The optimized structures are shown in Fig. 2, together with the corresponding interaction energies. Since the effects of electron correlations are known to increase with an increase of the size of molecular clusters, it is worthwhile to investigate these effects in the trimers. Therefore, additional geometry optimizations were carried out separately at the SCF level. The basis set used in the SCF calculations was 6-311++G(2d,2p). The optimized trimer structures at the SCF level are included in Fig. 2, together with the corresponding interaction energies.

The T-model potential predicted trimer A to be the most stable structure, with  $\Delta E_{\text{T-model}}$  of  $-77.49$  kJ/mol. Trimer A consists of six H-bonds. The H-bonds between molecules **a** and **b** are similar to those in dimer A, and the ones between molecules **b** and **c** are the same as in dimer B. The cyclic arrangement of the  $\text{N-H}\cdots\text{O}$  H-bonds, as in dimer D, is responsible for the attraction between molecules **a** and **c**. The second lowest-lying minimum energy geometry on the energy surface was predicted to be trimer B, with the interaction energy of  $-75.42$  kJ/mol. Trimer B can be built from dimers A and D. Molecule **b** bridges molecules **a** and **c** by three  $\text{N-H}\cdots\text{O}$  H-bonds. The T-model potential predicted trimer C to be only  $0.02$  kJ/mol less stable than trimer B. The H-bonds between molecules **a** and **b**, as well as molecules **b** and **c**, are similar to those in dimer B. The  $\text{NH}_2$  and  $\text{OH}$  groups in molecule **c** bridge molecules **a**

and **b**, through the  $\text{N-H}\cdots\text{O}$ ,  $\text{N-H}\cdots\text{N}$  and  $\text{O}\cdots\text{H-O}$  H-bonds. The T-model potential predicted a stacked H-bonded structure, trimer D in Fig. 2, to be another local minimum energy geometry. It possesses the interaction energy of  $-74.30$  kJ/mol. The H-bonds in trimer D are the same as those in dimers A and B. A cyclic arrangement of three  $\text{O-H}\cdots\text{O}$  H-bonds, as in the case of water [29], methanol [30] and phenol trimers [21] was found to be another local minimum energy geometry, trimer E in Fig. 2. The interaction energy in this case is  $-71.28$  kJ/mol. Based on the T-model results, the stability order for the trimers is written as:

T-model:  $A > B \geq C > D > E$

At the MP2/6-31G(d,p) level, Gaussian 94 predicted equilibrium geometries similar to the T-model results. The stability orders derived from MP2/6-31G(d,p) are:

MP2:  $A > D > E > B > C$   
 MP2CP:  $D > A > B > E > C$

It is seen that the stability orders obtained from the T-model, MP2 and MP2CP are not exactly the same. The discrepancies between the MP2 and MP2CP stability orders could be attributed to BSSE.  $\Delta E_{\text{BSSE}}$  for the trimers are, as expected, much larger than those for the dimers, ranging from about  $48$  kJ/mol for trimer E to about  $29$  kJ/mol for trimer D. The standard deviation of  $\Delta E_{\text{BSSE}}$  amounts to  $7.87$  kJ/mol. In order to systematically check the above stability orders, a further investigation, similar to that carried out for the dimers, must be made for the trimers. Trimer A was selected as a test case. The trimer structure obtained from MP2/6-31G(d,p) was reoptimized using MP2/6-311++G(2d,2p). The newly optimized geometry was virtually the same as the starting geometry. It is only about  $2$  kJ/mol more stable than the starting geometry. The energy values for the newly optimized geometry are shown in square brackets in Fig. 2.  $\Delta E_{\text{BSSE}}$  in this case was reduced to  $14.7$  kJ/mol, compared to  $47.15$  kJ/mol in the case of MP2/6-31G(d,p). These findings suggested one to improve the interaction energies of the trimers by following the same procedure as done for the dimers. Therefore, MP2/6-311++G(2d,2p) calculations on

the MP2/6-31G(d,p) optimized geometries were carried out. The energy results are given in parentheses in Fig. 2. The stability orders in this case are:

MP2:           D > A > E ≥ B > C  
 MP2CP:       D > A > B > E > C

$\Delta E_{\text{BSSE}}$  for MP2/6-311++G(2d,2p) are more isotropic, with the standard deviation of 0.78 kJ/mol.

At the SCF level, open-end H-bonded structures seem to be more favourable than the compact clusters. Starting from the compact trimers, A, B, C and E, the Berny optimization located only three different stacked H-bonded structures to be the minimum energy geometries. This indicates that the details of the SCF potential energy surface are completely different from those of the T-model and MP2. This is, certainly, due to the neglect of the effects of electron correlation in the SCF calculations. Starting from trimer A, the trimer built from dimers A and B was found to be the most stable at the SCF/6-311++G(2d,2p) level.  $\Delta E_{\text{SCFCP}}$  in this case is  $-51.94$  kJ/mol, compared to  $\Delta E_{\text{MP2CP}}$  of trimer A of  $-71.94$  kJ/mol, using the same basis set. This indicates that trimer A is stabilized by the dispersion energy of about  $-20$  kJ/mol. Trimer B consisting of dimers A and D is 6.39 kJ/mol less stable than the absolute minimum. The least stable trimers in this series are the ones built from dimers B. They possess  $\Delta E_{\text{SCFCP}}$  of about  $-42.5$  kJ/mol.  $\Delta E_{\text{BSSE}}$  at the SCF level are quite isotropic and not as large as those at the MP2 level. They amount to about 4 kJ/mol at most.

Before leaving the present section, several remarks should be made on the results reported here. First of all, the equilibrium geometries of the dimers and trimers deduced based on the T-model potential were shown to be acceptable. They are not much different from those obtained from the MP2 calculations. This suggests that, in the situation in which there are many possibilities to form H-bonded complexes, the T-model could serve as a primary search tool to explore the most probable absolute, as well as local minimum energy geometries on the potential energy surfaces. If the size of the molecule of interest is not too large, an ab initio supermolecular approach at higher levels of theory may follow, starting from the equilibrium geometries predicted by the

T-model potential. The combination of the T-model and ab initio supermolecular approach will help reduce computational time and resources in the study of structures and energetics of molecular clusters. It should also be stressed that small discrepancies between the T-model and MP2 results were as expected, since the T-model and MP2 are obviously based on different theories and approximations. The MP2 results showed that the 6-311G(d,p) basis set is quite accurate for the geometry optimization. However, in order to obtain reasonable interaction energy values, one has to minimize BSSE by increasing the size of the basis set, e.g. by adding diffuse functions as well as polarization functions in the MP2 calculations. The present study also illustrated that MP2/6-311++G(2d,2p) is a more appropriate choice for the investigation of the dimers and trimers of  $\text{NH}_2\text{OH}$ , since  $\Delta E_{\text{BSSE}}$  are quite small and isotropic.

#### 4. Molecular dynamics (MD) simulations of liquid $\text{NH}_2\text{OH}$

$\text{NH}_2\text{OH}$  is rather unstable in both liquid and solid phases. It is soluble in water, liquid ammonia and methanol. The melting and boiling points of  $\text{NH}_2\text{OH}$  are at 306 and 331 K, respectively [31]. Based on the T-model potential deduced in the previous section, properties of liquid  $\text{NH}_2\text{OH}$  were investigated by considering 512  $\text{NH}_2\text{OH}$  molecules confined in a cubic box subject to periodic boundary conditions. MD simulations were performed at 318 and 329 K. The liquid density was fixed at the experimental value of  $1.204$  g/cm<sup>3</sup> [31]. The box length corresponding to the experimental density was 28.56 Å. The cut-off radius was fixed at half of the box length. The long range Coulomb interactions were handled using the Ewald summation. The time step used in solving the equations of motion was 0.0005 ps. The equilibration of the liquid system at each temperature consumed about 12 000 MD steps. After equilibrations, the liquid properties were investigated by following the trajectories of molecules in 12 000 MD steps. Moldy program [32] was employed in the MD simulations. The force routine in Moldy was modified to handle the T-model potential.

Since the experimental data on structure of liquid  $\text{NH}_2\text{OH}$  are restricted, a similar H-bonded liquid

Table 2  
Potential energies ( $\Delta E$ ) and self-diffusion coefficients ( $D$ ) of liquid  $\text{NH}_2\text{OH}$  derived from MD with the T-model potential

Average temperature(K)	$\Delta E(\text{kJ/mol})$	$D(10^{-5} \text{ cm}^2\text{s}^{-1})$
318	- 65.55	0.82
329	- 63.89	1.22

should be chosen for comparison. Having comparable molecular weights, as well as functional groups,  $\text{CH}_3\text{OH}$  and  $\text{CH}_3\text{NH}_2$  could be selected as candidates. However, after a literature survey, it was found that  $\text{CH}_3\text{OH}$  is more appropriate since some characteristic physical properties of  $\text{CH}_3\text{OH}$  and  $\text{NH}_2\text{OH}$  are similar. There are also more theoretical and experimental data on  $\text{CH}_3\text{OH}$  in both gas and liquid states. Some important information which supported the selection of  $\text{CH}_3\text{OH}$  will be briefly summarized here.

Structures of liquid  $\text{CH}_3\text{OH}$  were reported based on MC [33,34] and MD [35–37], as well as X-ray diffraction techniques [38]. A direct analysis of the X-ray structure function led to the conclusion that the average number of nearest oxygen neighbors per oxygen atom lies between 1.40 and 1.55 [38]. The radial distribution functions obtained from X-ray studies of liquid  $\text{CH}_3\text{OH}$  indicated extensive zig-zag  $\text{O}-\text{H}\cdots\text{O}-\text{H}$  bonding chains [38], similar to those found in the solid. The dipole moment of  $\text{CH}_3\text{OH}$  is slightly smaller than water, 1.7 D [39]. The dielectric constant and boiling points are 33.6 and 337.8 K [39], respectively. The absolute minimum energy geometry of  $(\text{CH}_3\text{OH})_2$  was reported based on ab initio calculations at the SCF/CEP-31G(d,p) (Compact Effective Core Potential) level to be an open-chain  $\text{O}-\text{H}\cdots\text{O}-\text{H}$  bonded dimer, with the interaction energy of  $-17.22 \text{ kJ/mol}$  [40]. The value for MP2/CEP-31G(d,p) was  $-19.31 \text{ kJ/mol}$ .

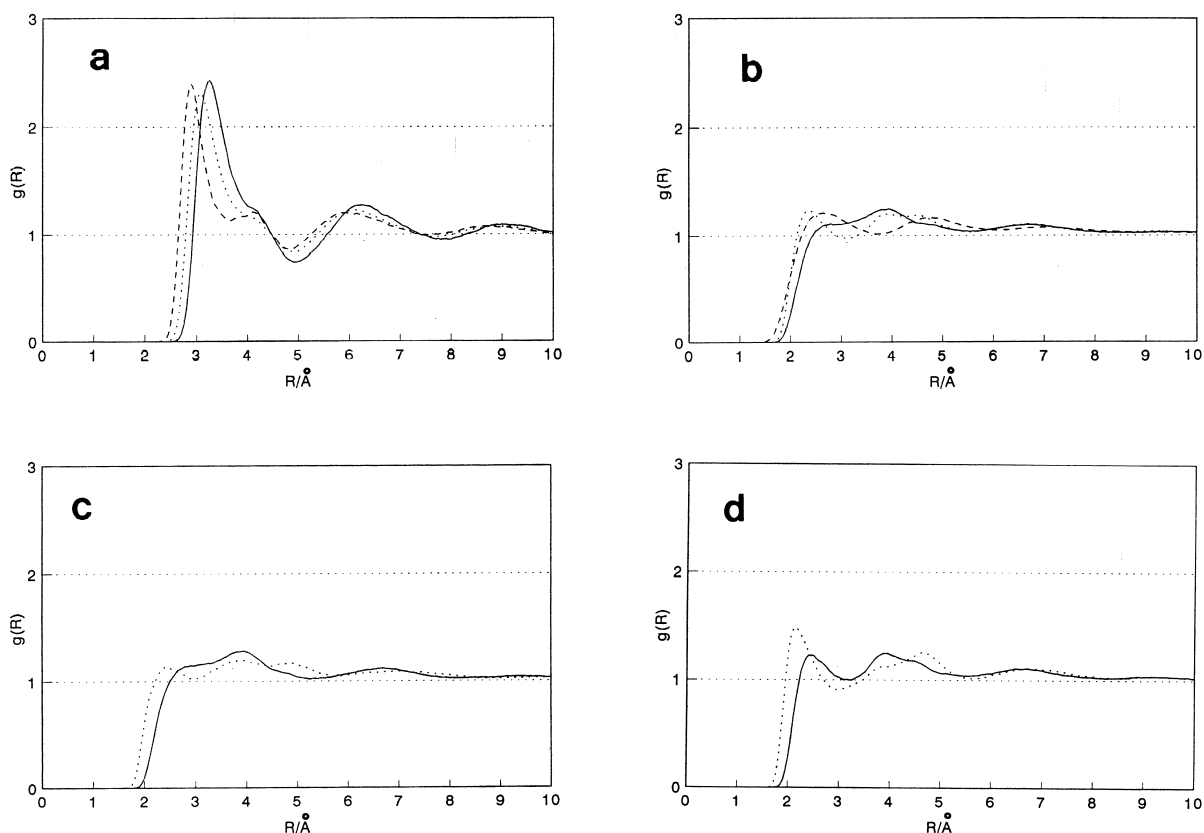


Fig. 3. Atom-atom pair correlation functions for liquid hydroxylamine, derived from MD at 329 K. (a) —  $g_{\text{NN}}(R_{\text{NN}})$ ; .....  $g_{\text{NO}}(R_{\text{NO}})$ ; ---  $g_{\text{OO}}(R_{\text{OO}})$ . (b) —  $g_{\text{NH}}(R_{\text{NH}})$ ; .....  $g_{\text{OH}}(R_{\text{OH}})$ ; ---  $g_{\text{HH}}(R_{\text{HH}})$ . (c) —  $g_{\text{NH}}^{\text{N}}(R_{\text{NH}}^{\text{N}})$ ; .....  $g_{\text{NH}}^{\text{O}}(R_{\text{NH}}^{\text{O}})$ . (d) —  $g_{\text{OH}}^{\text{N}}(R_{\text{OH}}^{\text{N}})$ ; .....  $g_{\text{OH}}^{\text{O}}(R_{\text{OH}}^{\text{O}})$ .

Weak C–H···O H-bonds were also observed around the methyl group [40]. This suggested the possibility to find a head-to-tail arrangement of O–C–H···O–C–H H-bonded chains in the liquid. The association in the O–C–H···O–C–H H-bonded chain is expected to be weaker than the O–N–H···O–N–H H-bonded chain in liquid NH<sub>2</sub>OH.

The potential energies of liquid NH<sub>2</sub>OH at 318 and 329 K are listed in Table 2. MD predicted the potential energy of the liquid at 318 K to be  $-65.55$  kJ/mol, comparable with the experimental heat of sublimation of  $64.1$  kJ/mol [41]. The value for solid CH<sub>3</sub>OH is  $37.4$  kJ/mol [39]. This indicates slightly weaker intermolecular interactions in the condensed phases for CH<sub>3</sub>OH.

Since the structure and peak locations of  $g_{ij}(R_{ij})$  are quite similar at both temperatures, only the ones at 318 K are discussed in detail.  $g_{ij}(R_{ij})$  are shown in Fig. 3. The structure of liquid NH<sub>2</sub>OH could be deduced from  $g_{\text{NN}}(R_{\text{NN}})$ ,  $g_{\text{NO}}(R_{\text{NO}})$  and  $g_{\text{OO}}(R_{\text{OO}})$ , and the average H-bonded structures could be inferred from  $g_{\text{NH}}(R_{\text{NH}})$  and  $g_{\text{OH}}(R_{\text{OH}})$ .

$g_{\text{NN}}(R_{\text{NN}})$ ,  $g_{\text{NO}}(R_{\text{NO}})$  and  $g_{\text{OO}}(R_{\text{OO}})$  show a similar peak structure, that is, the main peak is accompanied by a small shoulder at a slightly longer distance. Integrations of  $g_{\text{NN}}(R_{\text{NN}})$ ,  $g_{\text{NO}}(R_{\text{NO}})$  and  $g_{\text{OO}}(R_{\text{OO}})$  to their first minimum indicated that there are 11–12 NH<sub>2</sub>OH molecules in the first solvation shell. For  $g_{\text{NN}}(R_{\text{NN}})$ , the main peak, the shoulder and the first minimum are seen at  $R_{\text{NN}} = 3.20, 4.05$  and  $4.90$  Å, respectively. The main peak could be attributed to, either the N–H···N H-bonds, similar to those found in dimer B, or the N–N non-bond distances as in dimers A and D. The shoulder at  $4.05$  Å could be compared with the N···N distance, not involved in H-bond formation (see dimers C and E). Integration of  $g_{\text{NN}}(R_{\text{NN}})$  to the first maximum yielded the average number of nearest nitrogen neighbors ( $n_{\text{NN}}(R_{\text{NN}})$ ) to be about two. For  $g_{\text{NO}}(R_{\text{NO}})$ , the main peak and the shoulder are seen at  $R_{\text{NO}} = 3.05$  and  $4.10$  Å, respectively. The main peak is compatible with both O–H···N and N–H···O H-bond distances. Integration of  $g_{\text{NO}}(R_{\text{NO}})$  to the first maximum yielded 1.7 molecules in closest contact. The main peak and the shoulder of  $g_{\text{OO}}(R_{\text{OO}})$  are located at  $R_{\text{OO}} = 2.85$  and  $4.05$  Å, respectively. They could be assigned to the O–H···O H-bond and O···O non-H-bond distances, respectively. The main peak of  $g_{\text{OO}}(R_{\text{OO}})$  is located at approximately the same

position as in the case of liquid CH<sub>3</sub>OH [38]. Integration of  $g_{\text{OO}}(R_{\text{OO}})$  to the first maximum suggested about 1.3 molecules in closest contact. Since  $g_{\text{NN}}(R_{\text{NN}})$ ,  $g_{\text{NO}}(R_{\text{NO}})$  and  $g_{\text{OO}}(R_{\text{OO}})$  show similar peak structures and peak heights, one expects almost equal probability of finding N···N, N···O and O···O in the range which could form H-bonds.

It was pointed out based on the X-ray diffraction analysis of liquid CH<sub>3</sub>OH [38] that the average number of nearest oxygen neighbors ( $n_{\text{OO}}(R_{\text{OO}})$ ) could be qualitatively related to the length of the O–H···O H-bonded chains.  $n_{\text{OO}}(R_{\text{OO}}) = 2$  implies the presence of infinite zig-zag H-bonded chains.  $n_{\text{OO}}(R_{\text{OO}})$  is reduced to 1 in the dimeric form. For liquid CH<sub>3</sub>OH, the value was determined to lie between 1.4 and 1.5 [38]. Since  $n_{\text{OO}}(R_{\text{OO}})$  is 1.3 for liquid NH<sub>2</sub>OH, one might expect that liquid NH<sub>2</sub>OH and CH<sub>3</sub>OH could possess similar O–H···O H-bonded networks. The relationship between  $n_{\text{OO}}(R_{\text{OO}})$  and the number of monomers in the O–H···O H-bonded chains ( $M$ ) was suggested [38] to be  $n_{\text{OO}}(R_{\text{OO}}) = 2(M - 1)/M$ . The number of monomers in the H-bonded chains for liquid CH<sub>3</sub>OH was inferred from X-ray diffraction [38] to be between 3 and 4, and that deduced from computer simulations was fewer than 10 monomers [36]. If this relationship is correct,  $M$ , for liquid NH<sub>2</sub>OH, is about 3, and one could expect open-chain H-bonds to dominate the liquid structure.

In order to distinguish between the H-bond and the non-H-bond N···N distances,  $g_{\text{NH}}(R_{\text{NH}})$  was investigated in detail. Since the total  $g_{\text{NH}}(R_{\text{NH}})$  in Fig. 3(b) shows nearly no structure, a refinement was made. In this case  $g_{\text{NH}}(R_{\text{NH}})$  for the N–H···N H-bonds and that for the O–H···N H-bonds were filtered out of the total  $g_{\text{NH}}(R_{\text{NH}})$ . They are  $g_{\text{NH}}(R_{\text{NH}}^{\text{N}})$  and  $g_{\text{NH}}(R_{\text{NH}}^{\text{O}})$  in Fig. 3(c), respectively.  $g_{\text{NH}}(R_{\text{NH}}^{\text{N}})$  shows a small shoulder and a hump at  $2.75$  and  $3.90$  Å, respectively. The distances seem to be too long to compare with the dimers in Fig. 1. A small hump is seen at  $2.40$  Å for  $g_{\text{NH}}(R_{\text{NH}}^{\text{O}})$ . The location of the hump seems also to be a little too far to match exactly with the O–H···N H-bond distance in dimer A. The shoulder of  $g_{\text{NH}}(R_{\text{NH}}^{\text{N}})$  and the hump of  $g_{\text{NH}}(R_{\text{NH}}^{\text{O}})$  could, however, be attributed to the N–H···N and O–H···N H-bonds, in which the N–H, as well as O–H, bonds deviate considerably from the N···N and O···N axes, respectively. The deviation from the linearity of the H-bond protons suggests that the cyclic arrangements of

H-bonds, as in the dimers in Fig. 1, might not dominate the liquid structure.  $\text{NH}_2\text{OH}$  tends to make use of all available proton donors and acceptors to form, as extensive as possible, H-bonded networks with its neighbors. The situation is similar to formamide [18], in which the cyclic dimer is energetically more stable than the linear dimer in the gas phase, but it is found much less often in the liquid.

The existence of the cyclic arrangement of O–H $\cdots$ N H-bonds could be further discussed based on  $g_{\text{NH}}(R_{\text{NH}}^{\text{O}})$  and  $g_{\text{NH}}(R_{\text{NH}}^{\text{N}})$ . Since the first hump of  $g_{\text{NH}}(R_{\text{NH}}^{\text{O}})$  is comparable with the shoulder of  $g_{\text{NH}}(R_{\text{NH}}^{\text{N}})$ , the probability of finding O–H $\cdots$ N and N–H $\cdots$ O H-bonds is expected to be roughly the same. This confirms that the majority of the H-bonds in the liquid are not the cyclic O–H $\cdots$ N H-bonds as in dimer A.

For  $g_{\text{OH}}(R_{\text{OH}})$ , only the main peak is seen at 2.35 Å. In order to distinguish between O $\cdots$ H–O and O $\cdots$ H–N H-bonds,  $g_{\text{OH}}(R_{\text{OH}}^{\text{O}})$  and  $g_{\text{OH}}(R_{\text{OH}}^{\text{N}})$  were filtered out of  $g_{\text{OH}}(R_{\text{OH}})$ . The main peak of  $g_{\text{OH}}(R_{\text{OH}}^{\text{O}})$  is seen at 2.15 Å. This could be assigned to the H $\cdots$ O distance in O–H $\cdots$ O H-bonds. Since the main peak of  $g_{\text{OH}}(R_{\text{OH}}^{\text{O}})$  is the most structured, compared to all others  $g_{\text{XH}}(R_{\text{XH}}^{\text{Y}})$  (where X and Y are O or N), one might conclude that the O–H $\cdots$ O H-bonds slightly dominate the liquid structure. This seems to support the previous suggestion that the O–H $\cdots$ O H-bonded networks in liquid  $\text{NH}_2\text{OH}$  and  $\text{CH}_3\text{OH}$  are quite similar and dominate the liquid structure.

At this point, one might conclude that, although the cyclic arrangements of H-bonds are energetically more favourable in the dimers, there is no direct evidence showing their existence in an appreciable amount in the liquid. The results in this section suggest further that, all types of H-bonds, such as O–H $\cdots$ N, O–H $\cdots$ O, N–H $\cdots$ N as well as N–H $\cdots$ O could be present in the liquid, with a slightly higher possibility for O–H $\cdots$ O.

Comparison of the structure of liquid  $\text{NH}_2\text{OH}$  derived from the present MD and the previous MC [11] reveals both similarity and discrepancy. The peak locations of  $g_{ij}(R_{ij})$  are slightly different. The main peak of  $g_{\text{OO}}(R_{\text{OO}})$  derived from MC is split and about 30% lower than those of  $g_{\text{NN}}(R_{\text{NN}})$  and  $g_{\text{NO}}(R_{\text{NO}})$ . The first solvation shell was predicted by MC to contain 13  $\text{NH}_2\text{OH}$  molecules, from which four are the closest neighbors. The number of molecules in the

first shell is compatible with the present results. The first solvation shell derived from MC is, however, slightly larger than that from MD.  $g_{\text{OH}}(R_{\text{OH}}^{\text{O}})$  and  $g_{\text{NH}}(R_{\text{NH}}^{\text{O}})$  from MC are rather structured. They show slightly higher probability of finding O–H $\cdots$ N compared to O–H $\cdots$ O, whereas those from the present MD show slightly higher probability for O–H $\cdots$ O. Both MD and MC suggested a possibility to find the N–H $\cdots$ O and N–H $\cdots$ N H-bonds in the liquid. However, they seem to rule out the possibility to find cyclic dimers in the liquid.

The self-diffusion coefficients (D) derived from MD were reported in Table 2. The value at 329 K is  $1.22 \times 10^{-5} \text{ cm}^2/\text{s}^{-1}$ . The experimental values for liquid  $\text{CH}_3\text{OH}$  at the temperature range between 283 and 328 K were reported to be ranging from  $1.84 \times 10^{-5}$  to  $3.79 \times 10^{-5} \text{ cm}^2/\text{s}^{-1}$  [42]. The present MD results on liquid  $\text{NH}_2\text{OH}$  are compatible with the experimental values of liquid  $\text{CH}_3\text{OH}$ .

## 5. Conclusion

An intermolecular potential to describe the interaction between  $\text{NH}_2\text{OH}$  molecules was constructed based on the T-model. The computed T-model potential was applied in the investigation of equilibrium structures and interaction energies of  $(\text{NH}_2\text{OH})_2$  and  $(\text{NH}_2\text{OH})_3$ . The T-model potential predicted a cyclic arrangement of O–H $\cdots$ N H-bonds to be the absolute minimum energy geometry for the dimer. The dimer structure is compatible with the previous spectroscopic and ab initio results reported by Yeo et al. Other possible equilibrium dimer structures were also reported based on the T-model potential. This included the dimer with cyclic N–H $\cdots$ O H-bonds. Several trimer structures were suggested by the T-model potential to represent stationary points on the potential energy surface. The absolute minimum energy geometry of the trimer was found to be a compact cluster with six H-bonds. Some lowest-lying energy geometries of the dimers and trimers predicted by the T-model potential were re-examined using ab initio calculations at the MP2 level, with the 6-311G(d,p) and 6-31G(d,p) basis sets for the dimers and trimers, respectively. The energy results were improved by increasing the size of the basis set to 6-311++G(2d,2p). Starting from the equilibrium

structures of the dimers and trimers, predicted by the T-model potential, the Berny optimization routine in Gaussian 94 located stationary points which were, in general, not far from the initial structures. Although the stability orders for the dimers and trimers, deduced from the T-model and MP2, were not exactly the same, one might conclude that both methods yield similar and reasonable potential energy surfaces for the dimers and trimers. Small discrepancies were expected since the T-model and MP2 are based on different theories and approximations. It was proposed in the present study that the T-model could act as a primary search tool to explore all possible equilibrium structures of molecular clusters. If the molecules under consideration are not too large, more accurate results could be supplied by ab initio calculations in a supermolecular approach, starting from the T-model results. This combination will help reduce computational resources in the investigations. In the situation in which ab initio calculations could not be made easily on the clusters, the T-model has been proved to be quantitatively an acceptable choice. At the SCF level, open-end H-bonded structures seem to be more favourable than the compact H-bonded clusters. It was shown in the present study that the effects of electron correlation play an important role in the association of the compact H-bonded clusters.

Liquid  $\text{NH}_2\text{OH}$  was studied by MD at 318 and 329 K. The structure of liquid  $\text{NH}_2\text{OH}$  is quite similar to liquid  $\text{CH}_3\text{OH}$ . The MD results showed a slightly higher possibility of finding the  $\text{O}-\text{H}\cdots\text{O}$  H-bond compared to  $\text{O}-\text{H}\cdots\text{N}$  H-bond in the liquid. The present MD and the previous MC results seem to rule out the possibility of finding cyclic arrangement of H-bonds in the liquid.

### Acknowledgements

The author is indebted to the High-Performance Computer Center (HPCC) under the National Electronic and Computer Technology Center (NECTEC) in Bangkok for the CPU time in Silicon Graphics Power Challenge and Cray YMP-EL98 computers. Large parts of the calculations were performed at the DEC alpha 4710 and DEC alpha 600/5-266 at the School of Chemistry, Suranaree University of Technology, Thailand. The author would also like to thank Prof.

K. Haller at the School of Chemistry, Suranaree University of Technology, for reading the manuscript.

### References

- [1] G.A. Yeo, T.A. Ford, *Theor. Chim. Acta* 81 (1992) 255.
- [2] G.A. Yeo, T.A. Ford, *J. Chem. Soc. Faraday Trans.* 86 (1990) 3067.
- [3] G.A. Yeo, T.A. Ford, *Chem. Phys. Lett.* 178 (1991) 266.
- [4] G.A. Yeo, T.A. Ford, *Spectrochim. Acta* 50A (1994) 5.
- [5] G.A. Yeo, T.A. Ford, *J. Mol. Struct.* 141 (1986) 331.
- [6] G.A. Yeo, T.A. Ford, *J. Mol. Struct.* 270 (1992) 417.
- [7] G.A. Yeo, T.A. Ford, *J. Mol. Struct.* 217 (1990) 307.
- [8] R.E. Brown, Q. Zhang, R.J. Bartlett, *J. Am. Chem. Soc.* 113 (1991) 5248.
- [9] J.L. Scott, D. Luckhaus, S.S. Brown, F.F. Crim, *J. Chem. Phys.* 102 (1995) 675.
- [10] Y. Michopoulos, P. Botschwina, B.M. Rode, *Z. Naturforsch.* 46A (1991) 32.
- [11] Y. Michopoulos, B.M. Rode, *Physica Scripta* T38 (1991) 84.
- [12] S. Tsunekawa, *J. Phys. Soc. Japan* 33 (1972) 167.
- [13] H.J. Boehm, R. Ahlrichs, *J. Chem. Phys.* 77 (1982) 2028.
- [14] K.P. Sagarik, R. Ahlrichs, S. Brode, *Mol. Phys.* 57 (1986) 1247.
- [15] K.P. Sagarik, R. Ahlrichs, *Chem. Phys. Lett.* 131 (1986) 74.
- [16] H.J. Boehm, C. Meissner, R. Ahlrichs, *Mol. Phys.* 53 (1984) 651.
- [17] H.J. Boehm, R. Ahlrichs, *Mol. Phys.* 55 (1985) 1159.
- [18] K.P. Sagarik, R. Ahlrichs, *J. Chem. Phys.* 86 (1987) 5117.
- [19] K.P. Sagarik, V. Pongpituk, S. Chiyapongs, P. Sisot, *Chem. Phys.* 156 (1991) 439.
- [20] K.P. Sagarik, E. Spohr, *Chem. Phys.* 199 (1995) 73.
- [21] K.P. Sagarik, P. Asawakun, *Chem. Phys.* 219 (1997) 173.
- [22] D.E. Williams, R.R. Weller, *J. Am. Chem. Soc.* 105 (1983) 4143.
- [23] C.M. Breneman, K.B. Wiberg, *J. Comput. Chem.* 11 (1990) 361.
- [24] S. Tsunekawa, *J. Phys. Soc. Japan* 33 (1972) 167.
- [25] J.B. Foresman, A. Frisch, *Exploring Chemistry with Electronic Structure Methods*, Gaussian, Inc., Pittsburgh, 1996.
- [26] H.B. Schlegel, *J. Comput. Chem.* 3 (1982) 214.
- [27] M.J. Frisch, G.W. Trucks, H.B. Schlegel, P.M.W. Gill, B.G. Johnson, M.A. Robb, J.R. Cheeseman, T. Keith, G.A. Petersson, J.A. Montgomery, K. Raghavachari, M.A. Al-Laham, V.G. Zakrzewski, J.V. Ortiz, J.B. Foresman, J. Cioslowski, B.B. Stefanov, A. Nanayakkara, M. Challacombe, C.Y. Peng, P.Y. Ayala, W. Chen, M.W. Wong, J.L. Andres, E.S. Replogle, R. Gomperts, R.L. Martin, D.J. Fox, J.S. Binkley, D.J. Defrees, J. Baker, J.P. Stewart, M. Head-Gordon, C. Gonzalez, J.A. Pople, Gaussian, Inc., Pittsburgh, PA, 1995.
- [28] S.F. Boys, F. Bemardi, *Mol. Phys.* 19 (1970) 553.
- [29] S. Leutwyler, T. Buergi, M. Schuetz, A. Taylor, *Faraday Discuss.* 97 (1994) 285.
- [30] O. Mo, M. Yanez, J. Elguero, *J. Mol. Struct. (Theochem)* 314 (1994) 73.

- [31] M. Windholz (Ed.), *The Merck Index*, Merck and Co. Inc., Rahway, NJ, 1983.
- [32] K. Refson, *Moldy User's Manual*, Department of Earth Science, Oxford University, 1996.
- [33] W.L. Jorgensen, *J. Am. Chem. Soc.* 102 (1980) 543.
- [34] W.L. Jorgensen, *J. Am. Chem. Soc.* 103 (1981) 341.
- [35] M. Haughney, M. Ferrario, I.R. McDonald, *Mol. Phys.* 58 (1986) 849.
- [36] M. Haughney, M. Ferrario, I.R. McDonald, *J. Phys. Chem.* 91 (1987) 4934.
- [37] G. Palinkas, E. Hawlicka, K. Heinzinger, *J. Phys. Chem.* 91 (1987) 4334.
- [38] M. Magini, G. Paschina, G. Piccaluga, *J. Chem. Phys.* 77 (1982) 2051.
- [39] J.A. Dean, *Lange's Handbook of Chemistry*, 4th Ed., McGraw-Hill, New York, 1992.
- [40] E.H.S. Anwender, M.M. Probst, B.M. Rode, *Chem. Phys.* 166 (1992) 341.
- [41] R.A. Back, J. Betts, *Can. J. Chem.* 43 (1965) 2157.
- [42] R.L. Hurle, L.A. Woolf, *Aust. J. Chem.* 33 (1980) 1947.